

Low and intermediate energy electron collisions with the C_2^- molecular anion

Gabriela Halmová[†], J.D. Gorfinkiel* and Jonathan Tennyson[†]

[†] Department of Physics and Astronomy, University College London, Gower St., London WC1E 6BT, UK

* Department of Physics and Astronomy, The Open University, Walton Hall, MK7 6AA Milton Keynes, UK

Abstract. Calculations are presented which use the molecular R-matrix with pseudo-states (MRMPS) method to treat electron impact electron detachment and electronic excitation of the carbon dimer anion. Resonances are found above the ionisation threshold of C_2^- with $^1\Sigma_g^+$, $^1\Pi_g$ and $^3\Pi_g$ symmetry. These are shape resonances trapped by the effect of an attractive polarisation potential competing with a repulsive Coulomb interaction. The Π_g resonances are found to give structure in the detachment cross section similar to that observed experimentally. Both excitation and detachment cross sections are found to be dominated by large impact parameter collisions whose contribution is modelled using the Born approximation.

1. Introduction

The carbon dimer anion is unusual among small anions in having bound electronically excited states. In addition electron scattering experiments performed in storage rings showed that C_2^- was one of a number of diatomic anions which, at least temporarily, are able to bind an additional electron leading to pronounced resonance structures in their measured cross sections (Andersen et al. 1996, Pedersen et al. 1998, Pedersen et al. 1999, Andersen et al. 2001, Collins et al. 2005). Similar results have also been found for systems containing the NO_2^- anion (?, ?). Given that the electron collisions occur against the background of a strongly repulsive Coulomb interaction, the occurrence of such resonance structures, which generally lie above the threshold for electron impact detachment, was unanticipated.

Theoretically the treatment of electron collisions with these diatomic anions is complicated by the need to treat the region immediately above the electron detachment threshold. Such intermediate energy calculations are difficult because of the presence of two continuum electrons. Previous theoretical studies have used bound state methods either unadapted (Pedersen et al. 1999) or with an absorbing potential (Sommerfeld et al. 1997, Sommerfeld et al. 2000) to study the continuum states of C_2^{2-} .

In a preliminary publication (Halmová & Tennyson 2008) we reported calculations using the molecular R-matrix with Pseudo-states (MRMPS) method (Gorfinkiel &

Tennyson 2004, Gorfinkiel & Tennyson 2005) which found a number of low-lying resonances. In this work we report fully on these calculations, including details of the models we tested to produce stable calculations and to demonstrate that our results are robust. In addition we report results for electron impact excitation of C_2^- .

2. Method

The R -matrix method is based on dividing coordinate space into two regions using a spherical boundary of radius a centred on the centre-of-mass of the target molecule (Burke & Berrington 1993, Burke & Tennyson 2005). The radius of the boundary is chosen so that the inner region contains all the electronic cloud of the target molecular states included in the calculation.

Inside the R -matrix sphere it is necessary to consider all short-range interactions between the N target electrons and the scattering one, such as exchange and electron correlation. In the outer region these effects are negligible so the scattering electron can be described as moving in the long-range multipole potential of the target molecule.

The accuracy of this method is strongly dependent on the representation of the problem in the inner region (Tennyson 1996*b*). In standard, low-energy calculations, the wave function for an $N+1$ electrons system in the inner region is given by the expansion:

$$\psi_k^{N+1} = \mathcal{A} \sum_{ij} a_{ijk} \Phi_i(\mathbf{x}_1 \dots \mathbf{x}_N) u_{ij}(\mathbf{x}_{N+1}) + \sum_i b_{ik} \chi_i(\mathbf{x}_1 \dots \mathbf{x}_{N+1}), \quad (1)$$

where k represents the k^{th} solution of the inner region Hamiltonian, \mathcal{A} is the antisymmetrisation operator, \mathbf{x}_i are the spatial and spin coordinates of electron i , u_{ij} are continuum orbitals (COs) which represent the scattering electron (Tennyson & Morgan 1999), a_{ijk} and b_{ik} are variational coefficients, Φ_i is the wave function of the i^{th} target state and χ_i are L^2 functions constructed from the target occupied and virtual molecular orbitals. These functions represent electron correlation and polarisation effects. In the first sum, the configuration state functions are constrained to give the correct (target) space and spin symmetry for the first N -electrons as well as the correct total, $N + 1$ electron space-spin symmetry. Doing this requires special consideration of phase effects due to electron ordering in the wave function (Tennyson 1997).

In the standard formulation of the R -matrix method all the solutions of the inner region problem are required to construct the R -matrix on the boundary (Burke & Berrington 1993). This presents a serious computational barrier for large calculations as diagonalising the entire Hamiltonian may not be feasible. For some of the calculations discussed below we used the partitioned R -matrix method (Tennyson 2004), which only requires the low-lying eigenvalues and which has been demonstrated to give good results for the electron – C_2^- problem (Tennyson & Halmová 2007).

Here we use the UK polyatomic R -matrix code (Morgan et al. 1997) rather than the specialised, Slater orbital-based diatomic code. This is because the MRMPS method described below relies on the use Gaussian Type Orbitals (GTOs) and is therefore only

implemented in this code. The highest symmetry available in the polyatomic code is D_{2h} which is a subgroup of the true $D_{\infty h}$ symmetry of C_2^- . All calculations presented here were performed in D_{2h} symmetry. In the polyatomic suite target, continuum and MRMPS pseudo-continuum orbitals are all represented by a linear combination of GTOs. The target wave functions are expanded as a linear combination of the configurations ϕ_k :

$$\Phi_i(\mathbf{x}_1 \dots \mathbf{x}_N) = \sum_k c_{ik} \phi_k(\mathbf{x}_1 \dots \mathbf{x}_N), \quad (2)$$

where the c_{ik} coefficients are determined by diagonalising the Hamiltonian of the molecular target. The quality of the target wave functions is dependent on the size of this expansion, as is indirectly, the quality of the scattering calculation (Tennyson 1996b).

The central idea of the MRMPS method is the augmentation of the close-coupling expansion (1) with extra ‘‘target’’ wave functions Φ_i that represent pseudo-states. Unlike the usual target wave functions, these pseudo-states are not approximations to true eigenstates of the target, but are used to represent a discretised version of the electronic continuum. These pseudo-states are obtained by diagonalising the target electronic Hamiltonian expressed in an appropriate basis of configurations, see below.

As we are considering an anionic target, there are a finite number of bound target electronic states: three in the case C_2^- . This means that, unlike previous MRMPS studies (Gorfinkiel & Tennyson 2004, Gorfinkiel & Tennyson 2005), the pseudo-states are expected to all lie above the threshold to ionisation (electron detachment) where they represent the discretised target continuum. Of course, as the pseudo-continuum orbitals are added to the target basis they also influence the representation of the target states. It is a standard and tested assumption of the R-matrix with pseudo-states method that electron impact ionisation cross sections can be obtained by summing the cross sections for excitation of pseudo-states which lie above the vertical excitation threshold (Bartschat & Bray 1996).

To generate configurations that describe an ionised target, the MRMPS method uses an extra set of orbitals called pseudo-continuum orbitals (PCOs). These orbitals are used to describe the ionised electron. The PCOs are expanded in terms an even-tempered basis set (Schmidt & Ruedenberg 1979) of GTOs centred at the centre of mass of the system. In this type of basis sets, the exponents of the GTOs follow:

$$\alpha_i = \alpha_0 \beta^{(i-1)}, \quad \beta > 1, \quad i = 1, \dots, L, \quad (3)$$

where by choosing different values of the parameters α_0 and β different basis sets can be systematically generated. This is useful for checking the convergence and stability of the calculation and, of particular importance here, identifying physical resonances as distinct from the pseudo-resonances which are a known artifact of the RMPS procedure (Bartschat et al. 1996).

Given that the COs are also represented by GTOs, to avoid problems with linear dependence it is necessary to remove those CO basis functions from the set whose exponents are greater than α_0 . Even after this condition care has to be taken to ensure

that the three basis sets (target, CO and PCO) give a linearly independent set of orbitals. To do this the PCOs are first Schmidt orthogonalised to the target molecular orbitals (MOs) and then symmetric orthogonalised among themselves. At this stage those orbitals with eigenvalues of the overlap matrix less than a deletion threshold δ , here taken as 4×10^{-6} , were assumed to be linearly dependent and were removed from the basis. This procedure is repeated for the COs, here using $\delta = 2 \times 10^{-6}$.

3. Calculations

3.1. Target representation

The starting point for the present calculations was our previous study of the electron – C_2 system (Halmova et al. 2006). In that work the states of C_2 were represented using the double-zeta plus polarisation (DZP) Gaussian basis set of Dunning (1970), natural orbitals and a complete active space configuration interaction (CAS-CI) in which the four 1s electrons were frozen in the $1\sigma_g$ and $1\sigma_u$ orbitals, and the remaining eight electrons were freely distributed among the $2\sigma_g$, $3\sigma_g$, $2\sigma_u$, $3\sigma_u$, $1\pi_u$ and $1\pi_g$ orbitals giving configurations which can be written $(1\sigma_g 1\sigma_u)^4 (2\sigma_g 3\sigma_g 2\sigma_u 3\sigma_u 1\pi_u 1\pi_g)^8$. To treat C_2^- we added a PCO basis comprising 10 s, 10 p and 6 d orbitals. In this subsection all results presented used PCO exponents generated using $\alpha_0=0.17$ and $\beta=1.4$. The calculations presented here are for C_2^- in its equilibrium geometry for which $R = 2.396 a_0$ (Huber & Herzberg 1979).

The previous MRMPs studies considered electron impact ionisation of H_2 and H_3^+ (Gorfinkiel & Tennyson 2004, Gorfinkiel & Tennyson 2005), which are both two electron systems. In this case the construction of ionised target plus PCO configurations is straightforward. This is not so here where there are many possible configurations that could be selected. The need to (a) get a good representation of the (pseudo)-continuum, (b) get good energies and wave functions for the physical states of the target, (c) obtain a balanced description between the target and scattering calculations and (d) keep the whole calculation computationally tractable meant that considerable experimentation was required. Table 1 summarises the models, giving the target configurations used in (2), which were tested as part of the present study.

Besides choosing a basis set and a set of configurations, it is also necessary to build a set of target molecular orbitals. For standard scattering calculations these orbitals are normally ones associated with the N -electron target under consideration. However for calculations involving ionisation the final target state only has $N-1$ electrons; experience (Gorfinkiel & Tennyson 2004), echoed by tests performed as part of this work, has shown that use of orbitals associated with the ionised target gives best results. We therefore tested two sets of C_2 MOs, those generated from a self consistent field (SCF) calculation and natural orbitals (NOs) generated using the prescription given previously (Halmova et al. 2006).

Table 2 gives energies for states of C_2^- calculated with the various models and

Table 1. Configurations used in the various target models tested. N is the size of the resulting Hamiltonian matrix for 2A_g symmetry and PCO means pseudo continuum orbital.

Model	N	Configurations
1	1110	$(1\sigma_g 1\sigma_u)^4 (2\sigma_g 3\sigma_g 4\sigma_g 2\sigma_u 3\sigma_u 1\pi_u 1\pi_g)^9$ $(1\sigma_g 2\sigma_g 1\sigma_u 2\sigma_u 1\pi_u)^{12}$ (PCOs) ¹
2	140	$(1\sigma_g 2\sigma_g 1\sigma_u 2\sigma_u)^8 1\pi_u^4 (3\sigma_g 3\sigma_u 1\pi_g)^1$ $(1\sigma_g 2\sigma_g 1\sigma_u 2\sigma_u)^8 1\pi_u^3 (3\sigma_g 3\sigma_u 1\pi_g)^2$ $(1\sigma_g 2\sigma_g 1\sigma_u 2\sigma_u)^8 1\pi_u^4$ (PCOs) ¹ $(1\sigma_g 2\sigma_g 1\sigma_u 2\sigma_u)^8 1\pi_u^3 (3\sigma_g 3\sigma_u 1\pi_g)^1$ (PCOs) ¹
3	1600	$(1\sigma_g 1\sigma_u 2\sigma_g)^6 1\pi_u^4 (2\sigma_u 3\sigma_g 3\sigma_u 1\pi_g)^3$ $(1\sigma_g 1\sigma_u 2\sigma_g)^6 1\pi_u^3 (2\sigma_u 3\sigma_g 3\sigma_u 1\pi_g)^4$ $(1\sigma_g 1\sigma_u 2\sigma_g)^6 1\pi_u^4 (2\sigma_u 3\sigma_g 3\sigma_u 1\pi_g)^2$ (PCOs) ¹ $(1\sigma_g 1\sigma_u 2\sigma_g)^6 1\pi_u^3 (2\sigma_u 3\sigma_g 3\sigma_u 1\pi_g)^3$ (PCOs) ¹
4	425	$(1\sigma_g 1\sigma_u)^4 (2\sigma_g 3\sigma_g 2\sigma_u 3\sigma_u 1\pi_u 1\pi_g)^9$ $(1\sigma_g 2\sigma_g 1\sigma_u 2\sigma_u)^8 1\pi_u^4$ (PCOs) ¹ $(1\sigma_g 2\sigma_g 1\sigma_u 2\sigma_u)^8 1\pi_u^3 (3\sigma_g 3\sigma_u 1\pi_g)^1$ (PCOs) ¹
5	597	$(1\sigma_g 1\sigma_u)^4 (2\sigma_g 3\sigma_g 2\sigma_u 3\sigma_u 1\pi_u 1\pi_g)^9$ $(1\sigma_g 1\sigma_u)^4 (2\sigma_g 2\sigma_u 1\pi_u)^8$ (PCOs) ¹ $(1\sigma_g 1\sigma_u)^4 (2\sigma_g 2\sigma_u 1\pi_u)^7 (3\sigma_g 3\sigma_u 1\pi_g)^1$ (PCOs) ¹
6	3111	$(1\sigma_g 1\sigma_u)^4 (2\sigma_g 3\sigma_g 2\sigma_u 3\sigma_u 1\pi_u 1\pi_g)^9$ $(1\sigma_g 1\sigma_u)^4 (2\sigma_g 2\sigma_u 1\pi_u)^8$ (PCOs) ¹ $(1\sigma_g 1\sigma_u)^4 (2\sigma_g 2\sigma_u 1\pi_u)^7 (3\sigma_g 3\sigma_u 1\pi_g)^1$ (PCOs) ¹ $(1\sigma_g 1\sigma_u)^4 (2\sigma_g 2\sigma_u 1\pi_u)^6 (3\sigma_g 3\sigma_u 1\pi_g)^2$ (PCOs) ¹
7	20454	$(1\sigma_g 1\sigma_u 2\sigma_g)^6 (2\sigma_u 3\sigma_g 3\sigma_u 1\pi_g 1\pi_u)^7$ $(1\sigma_g 1\sigma_u 2\sigma_g)^6 (2\sigma_u 3\sigma_g 3\sigma_u 1\pi_g 1\pi_u)^6$ (PCOs) ¹
8	97500	$(1\sigma_g 1\sigma_u)^4 (2\sigma_g 3\sigma_g 4\sigma_g 2\sigma_u 3\sigma_u 1\pi_u 1\pi_g)^9$ $(1\sigma_g 1\sigma_u)^4 (2\sigma_g 3\sigma_g 4\sigma_g 2\sigma_u 3\sigma_u 1\pi_u 1\pi_g)^8$ (PCOs) ¹

orbitals sets. These can be compared with the results of our previous study (Halmova et al. 2006) which, once nuclear motion effects had been taken into account, gave good agreement with the experimental results reported in Huber & Herzberg (1979).

Considering each model in turn. Model 1 gave reasonable target energies but the pseudo-state configurations are very limited as they are obtain from a single electron in a PCO and a frozen target C_2 ; this treatment is not consistent with the CAS-CI representation of C_2^- . Model 2 is more consistent in that 8 electrons are frozen in all configurations. However this much more limited model gave poor energies for the target states; indeed with SCF MOs it did not even predict the correct ground state for C_2^- . Model 3 is built on Model 2 but with only 6 target electrons completely frozen; it gives rather a large scattering Hamiltonian and when tested did not give particularly good

Table 2. C_2^- ground state energies (negative numbers in E_h) and excitation energies (in eV) for different models and orbitals.

Model	X $^2\Sigma_g^+$		A $^2\Pi_u$		B $^2\Sigma_u^+$	
	SCF MOs	C_2 NOs	SCF MOs	C_2 NOs	SCF MOs	C_2 NOs
1	-75.61166	-	0.729	-	2.673	-
2	1.951	-75.53709	-75.56659	0.850	7.955	5.813
3	-75.59480	-75.58782	0.597	0.611	3.115	2.549
4	-75.60956	-75.60944	0.468	0.419	2.734	2.506
5	-75.62675	-	0.883	-	2.717	-
6	-75.65777	-	0.912	-	2.908	-
7	0.123	-75.71419	-75.66055	0.686	1.823	2.621
8	-75.72075		0.689		2.621	
<i>a</i>		-75.67213		0.557		2.355

^a Previous calculations (Halmova et al. 2006).

eigenphase sums. Model 4 was built as a hybrid between Models 1 and 2 using the target configurations from the former and pseudo-state configurations from the latter. This model gave good target energies and a relatively small Hamiltonian size for the scattering problem. This model formed the basis of our preliminary study (Halmová & Tennyson 2008) and became our workhorse for test calculations. Model 5 is a slightly enlarged version of model 4 and behaves similarly.

Use of the partitioned R-matrix method allowed us to explore target models which implied significantly larger Hamiltonians for the scattering problem. We therefore tested the effect of gradually expanding the CAS-CI used to generate the pseudo-states. The limit of the process is Model 8, in which the same extended CAS is used in both parts of the calculation. However, its corresponding scattering model is far too big to be tractable (see table 4) and was not pursued. Our attempts to construct intermediate models, gives numbers 6 and 7. Model 7 did not give good target energies. We therefore decided to concentrate on use of models 4, 5 and 6.

As can be seen from table 2, the use of C_2 SCF MOs gives results of similar quality to NOs, in contrast to more usual calculations where NOs give significantly better results. This is perhaps not surprising since the NOs were constructed to give a good representation of a range of electronically excited states of C_2 which is not our purpose here. The calculations reported below use SCF MOs unless otherwise stated.

There is one further target property which proved to be of considerable importance for the scattering calculations, that is the long range polarisability of C_2^- target. Gorfinkiel & Tennyson (2004) showed that the MRMPs method converges the long-range target polarisability in a way that standard close-coupling expansions do not. As is discussed below, a good representation of the polarisability is essential to get a good

Table 3. Isotropic polarisabilities of C_2^- in a_0^3 for different models, orbitals and PCO basis determined by (α_0, β) .

Model	$\alpha_0=0.17 \quad \beta=1.4$		$\alpha_0=0.15 \quad \beta=1.4$	$\alpha_0=0.17 \quad \beta=1.5$	$\alpha_0=0.17 \quad \beta=1.3$	
	SCF MOs	C_2 NOs			SCF MOs	SCF MOs
1	26.42					
2	28.58	109.51				
3	67.49	12.24				
4	32.24		32.48	31.24	31.98	18.80
5	25.00					
6	24.55					

physical model of the electron – molecular anion collision as it provides the dominant attractive term in the interaction.

Table 3 shows the isotropic polarisabilities predicted by various of our target models. We could find no literature value for this parameter. Indeed it is not straightforward to calculate it with standard electronic structure codes, we tried, as they are not generally set up to treat molecular anions. The table shows that the calculated polarisability is generally stable with changes to the PCO basis but not with other aspects of the target model. In part this is because both excited states of C_2^- are dipole allowed from the ground state and low-lying. This makes the calculated polarisability particularly sensitive to the transition dipole and precise excitation energies of these states. Our results suggest that the true polarisability of C_2^- at $R = 2.396 a_0$ is between 25 and 32 a_0^3 , of this less than 10 a_0^3 arises from coupling to the two physical electronically excited states of C_2^- .

So far we have concentrated on our calculations of the physical properties of the target. There is however one other property of importance for the scattering runs: the spectral coverage of the continuum by the pseudo-states. Figure 1 compares energy levels generated by various versions of Model 4. The behaviour shown here, that the energy levels are stable to choice of PCO basis but very sensitive to the target model used, was also shown in the other comparisons we made (Halmová 2008). A common feature of all the comparisons is the sparsity of states directly above ionisation. In principle one could get pseudo-states in this energy region by significantly expanding the R-matrix box size and the associated PCO basis; such a calculation was not deemed computationally tractable at present. However, as can be seen from the results presented below, our pseudo-state distributions lead to very small near-threshold electron impact detachment cross sections, which appears to be in agreement with the observations.

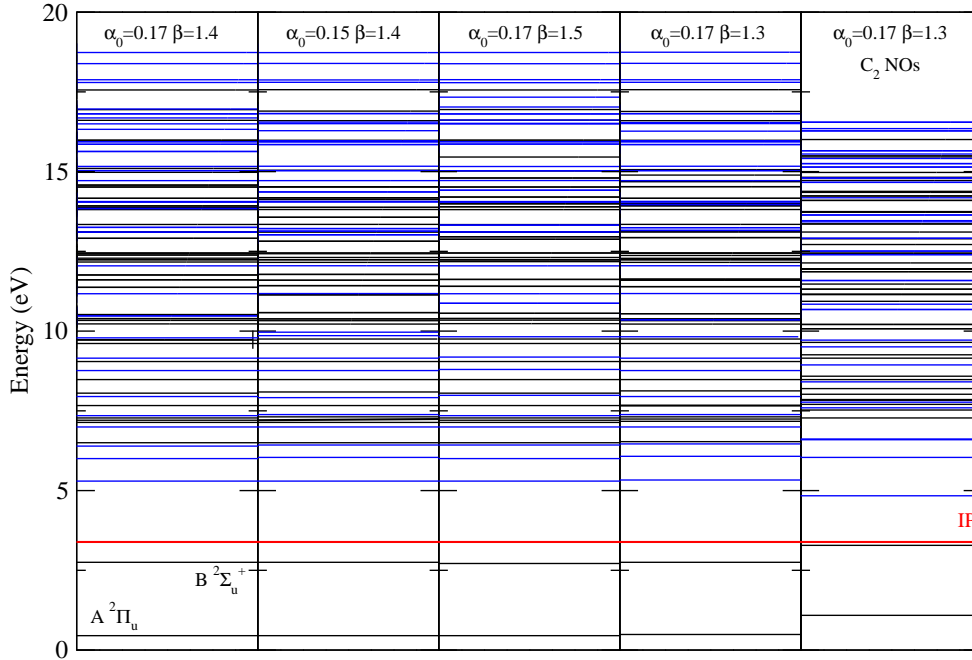


Figure 1. Target state distribution for C_2^- for Model 4 for various (α_0, β) values as indicated in the figure. Energies are relative to the $X \ ^3\Sigma_g^+$ ground state of C_2^- . SCF MOs of C_2 were used except where otherwise indicated. The horizontal line marked IP denotes the ionisation threshold.

3.2. Scattering model

Test calculations using Model 1 for R-matrix spheres of radius $a = 10 a_0$ and $13 a_0$ showed that $a = 10 a_0$ gave stable results and this was used for all further calculations. CO's were taken from Faure et al. (2002) with the largest exponent functions removed. This basis contains functions with ℓ up to 4 ie g orbitals. Use of two different sets of PCOs were tested:

4-14 a_g 2-7 b_{2u} 2-7 b_{3u} 1-4 b_{1g} 4-8 b_{1u} 2-5 b_{3g} 2-5 b_{2g} 1 a_u

4-24 a_g 2-10 b_{2u} 2-10 b_{3u} 1-7 b_{1g} 4-12 b_{1u} 2-8 b_{3g} 2-8 b_{2g} 1 a_u

in D_{2h} notation. The eigenphase calculated with the larger PCO set was slightly higher, so this was used for further calculation.

To go from the target models detailed above to the inner region R-matrix wave functions of (1) we followed the prescription developed previously (Tennyson 1996b) for standard R-matrix calculations. This prescription, which has been used successfully in many studies, is designed to provide a balanced treatment between the target, N -electron, and scattering, $N + 1$ -electron problems. Table 4 details the configurations generated for the $N+1$ -electron calculations associated with each of the models described above. Also given is the size of the final Hamiltonian, a crucial parameter in determining the tractability of the calculation. Although our Hamiltonian construction algorithm is very efficient meaning the computational demands of this step of the calculation only depend weakly on the number of target states (and pseudo-states) included in

the expansion (Tennyson 1996a), the diagonalisation step still represents a major bottleneck. As a result, the largest previously published molecular R-matrix calculation was restricted to $N \sim 28000$ (Rozum et al. 2003).

Model 8 gives an extremely large final step Hamiltonians and no attempt was made to actually solve for it. Many calculations were performed for Models 1 to 6 for testing purposes. Calculations using the partitioned R-matrix method (Tennyson 2004) explicitly considered the lowest 1000 solutions which were found to be sufficient to span scattering energies up to about 40 eV.

Scattering calculations were performed for both singlet and triplet symmetries. After some experimentation it was decided to include 114 target states in the final close-coupling expansion. This number is evaluated in D_{2h} symmetry so counts states which are degenerate in $D_{\infty h}$ symmetry twice. 66 of these states are doublets of which the lowest 3 are the physical states of C_2^- . The 48 quartet states only couple to triplet calculations. These states span energies up to about 19 eV above the target ground state for both Models 4, 5 and 6.

Outer region calculations were performed by propagating the R-matrices to $100 a_0$ and then matching to asymptotic Coulomb functions. This large number of states makes the outer calculations slow compared to standard R-matrix calculations but we were still able to generate results for sufficient energies to map out the various resonance structures, both real and pseudo.

3.3. Born Approximation

The interaction between the scattering electron and the C_2^- anion is long-range and repulsive. It can therefore be expected that many of the collisions will occur with a large impact parameter. Such collisions are not well represented in the calculations described above, all of which use a CO basis set and hence partial wave expansion truncated at $\ell = 4$. However collisions with high values of electron angular momentum ($\ell > 4$) are amenable to a much simpler treatment since in these collisions the scattering electron can be assumed not to penetrate the charge cloud of the C_2^- target. Under these circumstances the collision cross sections are determined by purely long-range effects.

To allow the important effect of collisions with $\ell > 4$ in the inelastic cross sections presented here, we used a simple top-up procedure based on the Born approximation (Baluja et al. 2001). There are a number of ways applying such a Born top-up procedure but since C_2^- is non-polar, meaning rotational effects will be small, and the non-resonant cross sections at low ℓ are very small, meaning that interference effects for these ℓ 's will not be important, the simplest procedure based on the direct augmentation of the cross sections was used. This procedure was applied to electron impact electronic excitation of all physical and pseudo states which are dipole allowed, that is to all excitations to states of $^2\Sigma_u^+$ and $^2\Pi_u$ symmetry. Only transition dipole moments were considered for the long-range potential. For the pseudo-states this extra excitation cross sections were taken as supplementing the electron impact detachment cross sections. This increase

Table 4. Configurations used for the various scattering models tested. N is the size of the resulting Hamiltonian matrix with 1A_g symmetry and PCO means pseudo continuum orbital and CO means continuum orbital.

Model	N	Configurations
1	21705	$(1\sigma_g 1\sigma_u)^4 (2\sigma_g 3\sigma_g 4\sigma_g 2\sigma_u 3\sigma_u 1\pi_u 1\pi_g)^9$ (COs) ¹ $(1\sigma_g 2\sigma_g 1\sigma_u 2\sigma_u 1\pi_u)^{12}$ (PCOs) ¹ (COs) ¹ $(1\sigma_g 1\sigma_u)^4 (2\sigma_g 3\sigma_g 4\sigma_g 2\sigma_u 3\sigma_u 1\pi_u 1\pi_g)^{10}$ $(1\sigma_g 2\sigma_g 1\sigma_u 2\sigma_u 1\pi_u)^{12}$ (PCOs) ² $(1\sigma_g 2\sigma_g 1\sigma_u 2\sigma_u 1\pi_u)^{12} (3\sigma_g 4\sigma_g 3\sigma_u 1\pi_g)^1$ (PCOs) ¹
2	6447	$(1\sigma_g 2\sigma_g 1\sigma_u 2\sigma_u)^8 1\pi_u^4 (3\sigma_g 3\sigma_u 1\pi_g)^1$ (COs) ¹ $(1\sigma_g 2\sigma_g 1\sigma_u 2\sigma_u)^8 1\pi_u^3 (3\sigma_g 3\sigma_u 1\pi_g)^2$ (COs) ¹ $(1\sigma_g 2\sigma_g 1\sigma_u 2\sigma_u)^8 1\pi_u^4$ (PCOs) ¹ (COs) ¹ $(1\sigma_g 2\sigma_g 1\sigma_u 2\sigma_u)^8 1\pi_u^3 (3\sigma_g 3\sigma_u 1\pi_g)^1$ (PCOs) ¹ (COs) ¹ $(1\sigma_g 2\sigma_g 1\sigma_u 2\sigma_u)^8 1\pi_u^4 (3\sigma_g 3\sigma_u 1\pi_g)^2$ $(1\sigma_g 2\sigma_g 1\sigma_u 2\sigma_u)^8 1\pi_u^4 (3\sigma_g 3\sigma_u 1\pi_g)^1$ (PCOs) ¹ $(1\sigma_g 2\sigma_g 1\sigma_u 2\sigma_u)^8 1\pi_u^4$ (PCOs) ² $(1\sigma_g 2\sigma_g 1\sigma_u 2\sigma_u)^8 1\pi_u^3 (3\sigma_g 3\sigma_u 1\pi_g)^2$ (PCOs) ¹ $(1\sigma_g 2\sigma_g 1\sigma_u 2\sigma_u)^8 1\pi_u^3 (3\sigma_g 3\sigma_u 1\pi_g)^1$ (PCOs) ²
3	52270	$(1\sigma_g 1\sigma_u 2\sigma_g)^6 1\pi_u^4 (2\sigma_u 3\sigma_g 3\sigma_u 1\pi_g)^3$ (COs) ¹ $(1\sigma_g 1\sigma_u 2\sigma_g)^6 1\pi_u^3 (2\sigma_u 3\sigma_g 3\sigma_u 1\pi_g)^4$ (COs) ¹ $(1\sigma_g 1\sigma_u 2\sigma_g)^6 1\pi_u^4 (2\sigma_u 3\sigma_g 3\sigma_u 1\pi_g)^2$ (PCOs) ¹ (COs) ¹ $(1\sigma_g 1\sigma_u 2\sigma_g)^6 1\pi_u^3 (2\sigma_u 3\sigma_g 3\sigma_u 1\pi_g)^3$ (PCOs) ¹ (COs) ¹ $(1\sigma_g 1\sigma_u 2\sigma_g)^6 1\pi_u^4 (2\sigma_u 3\sigma_g 3\sigma_u 1\pi_g)^4$ $(1\sigma_g 1\sigma_u 2\sigma_g)^6 1\pi_u^4 (2\sigma_u 3\sigma_g 3\sigma_u 1\pi_g)^3$ (PCOs) ¹ $(1\sigma_g 1\sigma_u 2\sigma_g)^6 1\pi_u^4 (2\sigma_u 3\sigma_g 3\sigma_u 1\pi_g)^2$ (PCOs) ² $(1\sigma_g 1\sigma_u 2\sigma_g)^6 1\pi_u^3 (2\sigma_u 3\sigma_g 3\sigma_u 1\pi_g)^4$ (PCOs) ¹ $(1\sigma_g 1\sigma_u 2\sigma_g)^6 1\pi_u^3 (2\sigma_u 3\sigma_g 3\sigma_u 1\pi_g)^3$ (PCOs) ²
4	6575	$(1\sigma_g 1\sigma_u)^4 (2\sigma_g 3\sigma_g 2\sigma_u 3\sigma_u 1\pi_u 1\pi_g)^9$ (COs) ¹ $(1\sigma_g 2\sigma_g 1\sigma_u 2\sigma_u)^8 1\pi_u^4$ (PCOs) ¹ (COs) ¹ $(1\sigma_g 2\sigma_g 1\sigma_u 2\sigma_u)^8 1\pi_u^3 (3\sigma_g 3\sigma_u 1\pi_g)^1$ (PCOs) ¹ (COs) ¹ $(1\sigma_g 1\sigma_u)^4 (2\sigma_g 3\sigma_g 2\sigma_u 3\sigma_u 1\pi_u 1\pi_g)^{10}$ $(1\sigma_g 2\sigma_g 1\sigma_u 2\sigma_u)^8 1\pi_u^4$ (PCOs) ² $(1\sigma_g 2\sigma_g 1\sigma_u 2\sigma_u)^8 1\pi_u^3 (3\sigma_g 3\sigma_u 1\pi_g)^2$ (PCOs) ¹ $(1\sigma_g 2\sigma_g 1\sigma_u 2\sigma_u)^8 1\pi_u^3 (3\sigma_g 3\sigma_u 1\pi_g)^1$ (PCOs) ²
5	12283	$(1\sigma_g 1\sigma_u)^4 (2\sigma_g 3\sigma_g 2\sigma_u 3\sigma_u 1\pi_u 1\pi_g)^9$ (COs) ¹ $(1\sigma_g 1\sigma_u)^4 (2\sigma_g 2\sigma_u 1\pi_u)^8$ (PCOs) ¹ (COs) ¹ $(1\sigma_g 1\sigma_u)^4 (2\sigma_g 2\sigma_u 1\pi_u)^7 (3\sigma_g 3\sigma_u 1\pi_g)^1$ (PCOs) ¹ (COs) ¹ $(1\sigma_g 1\sigma_u)^4 (2\sigma_g 3\sigma_g 2\sigma_u 3\sigma_u 1\pi_u 1\pi_g)^{10}$ $(1\sigma_g 1\sigma_u)^4 (2\sigma_g 2\sigma_u 1\pi_u)^8$ (PCOs) ² $(1\sigma_g 1\sigma_u)^4 (2\sigma_g 2\sigma_u 1\pi_u)^7 (3\sigma_g 3\sigma_u 1\pi_g)^2$ (PCOs) ¹ $(1\sigma_g 1\sigma_u)^4 (2\sigma_g 2\sigma_u 1\pi_u)^7 (3\sigma_g 3\sigma_u 1\pi_g)^1$ (PCOs) ²
6	12283	$(1\sigma_g 1\sigma_u)^4 (2\sigma_g 3\sigma_g 2\sigma_u 3\sigma_u 1\pi_u 1\pi_g)^9$ (COs) ¹ $(1\sigma_g 1\sigma_u)^4 (2\sigma_g 2\sigma_u 1\pi_u)^8$ (PCOs) ¹ (COs) ¹ $(1\sigma_g 1\sigma_u)^4 (2\sigma_g 2\sigma_u 1\pi_u)^7 (3\sigma_g 3\sigma_u 1\pi_g)^1$ (PCOs) ¹ (COs) ¹ $(1\sigma_g 1\sigma_u)^4 (2\sigma_g 2\sigma_u 1\pi_u)^6 (3\sigma_g 3\sigma_u 1\pi_g)^2$ (PCOs) ¹ (COs) ¹ $(1\sigma_g 1\sigma_u)^4 (2\sigma_g 3\sigma_g 2\sigma_u 3\sigma_u 1\pi_u 1\pi_g)^{10}$ $(1\sigma_g 1\sigma_u)^4 (2\sigma_g 2\sigma_u 1\pi_u)^8$ (PCOs) ² $(1\sigma_g 1\sigma_u)^4 (2\sigma_g 2\sigma_u 1\pi_u)^7 (3\sigma_g 3\sigma_u 1\pi_g)^2$ (PCOs) ¹ $(1\sigma_g 1\sigma_u)^4 (2\sigma_g 2\sigma_u 1\pi_u)^7 (3\sigma_g 3\sigma_u 1\pi_g)^1$ (PCOs) ²
7	823823	$(1\sigma_g 1\sigma_u 2\sigma_g)^6 (2\sigma_u 3\sigma_g 3\sigma_u 1\pi_g 1\pi_u)^7$ (COs) ¹ $(1\sigma_g 1\sigma_u 2\sigma_g)^6 (2\sigma_u 3\sigma_g 3\sigma_u 1\pi_g 1\pi_u)^6$ (PCOs) ¹ (COs) ¹ $(1\sigma_g 1\sigma_u 2\sigma_g)^6 (2\sigma_u 3\sigma_g 3\sigma_u 1\pi_g 1\pi_u)^8$ $(1\sigma_g 1\sigma_u 2\sigma_g)^6 (2\sigma_u 3\sigma_g 3\sigma_u 1\pi_g 1\pi_u)^7$ (PCOs) ¹ $(1\sigma_g 1\sigma_u 2\sigma_g)^6 (2\sigma_u 3\sigma_g 3\sigma_u 1\pi_g 1\pi_u)^6$ (PCOs) ² $(1\sigma_g 1\sigma_u)^4 (2\sigma_g 3\sigma_g 2\sigma_u 3\sigma_u 1\pi_u 1\pi_g)^{10}$ $(1\sigma_g 1\sigma_u)^4 (2\sigma_g 2\sigma_u 1\pi_u)^8$ (PCOs) ² $(1\sigma_g 1\sigma_u)^4 (2\sigma_g 2\sigma_u 1\pi_u)^7 (3\sigma_g 3\sigma_u 1\pi_g)^2$ (PCOs) ¹ $(1\sigma_g 1\sigma_u)^4 (2\sigma_g 2\sigma_u 1\pi_u)^7 (3\sigma_g 3\sigma_u 1\pi_g)^1$ (PCOs) ²
8	too big	$(1\sigma_g 1\sigma_u)^4 (2\sigma_g 3\sigma_g 4\sigma_g 2\sigma_u 3\sigma_u 1\pi_u 1\pi_g)^9$ (COs) ¹ $(1\sigma_g 1\sigma_u)^4 (2\sigma_g 3\sigma_g 4\sigma_g 2\sigma_u 3\sigma_u 1\pi_u 1\pi_g)^8$ (PCOs) ¹ (COs) ¹ $(1\sigma_g 1\sigma_u)^4 (2\sigma_g 3\sigma_g 4\sigma_g 2\sigma_u 3\sigma_u 1\pi_u 1\pi_g)^{10}$ $(1\sigma_g 1\sigma_u)^4 (2\sigma_g 3\sigma_g 4\sigma_g 2\sigma_u 3\sigma_u 1\pi_u 1\pi_g)^9$ (PCOs) ¹ $(1\sigma_g 1\sigma_u)^4 (2\sigma_g 3\sigma_g 4\sigma_g 2\sigma_u 3\sigma_u 1\pi_u 1\pi_g)^8$ (PCOs) ²

Table 5. Energy, E_r , and width, Γ , both in eV, of resonance states of C_2^{2-} ; our results are based calculations with $\alpha_0=0.17$ and $\beta=1.4$.

Previous work				Model 4		Model 5		Model 6		
Symmetry	E_r	Γ	ref	Symmetry	E_r	Γ	E_r	Γ	E_r	Γ
$^1\Sigma_g^+$	3.5	0.3	<i>a</i>	$^1\Sigma_g^+$	4.86	0.65	4.75	0.57	4.91	0.67
	10.0	2.1	<i>b</i>	$^1\Pi_g$	10.92	0.52	10.59	0.57	11.46	0.82
	10.0	3 – 4	<i>b</i>	$^3\Pi_g$	9.71	1.14	9.54	0.99	10.44	1.43

^a Theory (Sommerfeld et al. 2000).

^b Experiment (Andersen et al. 1996, Pedersen et al. 1998, Pedersen et al. 1999).

turns out to be substantial showing that the majority of this process does in fact occur through long-range collisions.

4. Results

A very large number of different calculations were attempted. For space reasons only those performed using Models 4, 5 and 6 will be reported in detail. As a major aim of this study was to characterise the resonances observed in the storage ring experiments, it is this aspect of the work we discuss first. We will then give our results for total cross sections for both electron impact electronic excitation and electron detachment.

4.1. Resonances

All models tested showed a $^1\Sigma_g^+$ resonance feature at about 5 eV. However only the more sophisticated models showed stable resonances in the energy region probed by the storage ring experiments.

Figure 2 gives a series of Model 4 calculations for $^2B_{3g}$ symmetry contribution to the total electron impact electron detachment cross section as a function of energy. Both singlet and triplet contributions are dominated by a series of resonance features: several narrow resonances which show a strong dependence on the PCO basis set parameters and a single broad resonance in each case. In contrast to the narrow resonances, the position and width of the broad resonance features is stable with respect to the choice of PCO basis; indeed even the calculation with $\alpha_0=0.17$ and $\beta=1.5$ which shows a much enhanced resonance structure, a known signature of a poorly converged PCO basis (Bartschat et al. 1996), gives a similar resonance to the other calculations. Figure 3 gives a similar comparison for the total electron impact detachment cross section where again both the singlet and triplet resonance features are clearly visible. The poorer quality of the calculation based on the use of C_2 NOs can clearly be seen.

Inspection of plots of eigenphase sums (not given), showed one further clear resonance at energies just above the ionisation threshold of $^1\Sigma_g^+$ symmetry. Parameters for this resonance and the ones near 10 eV were obtained by fitting their eigenphases to

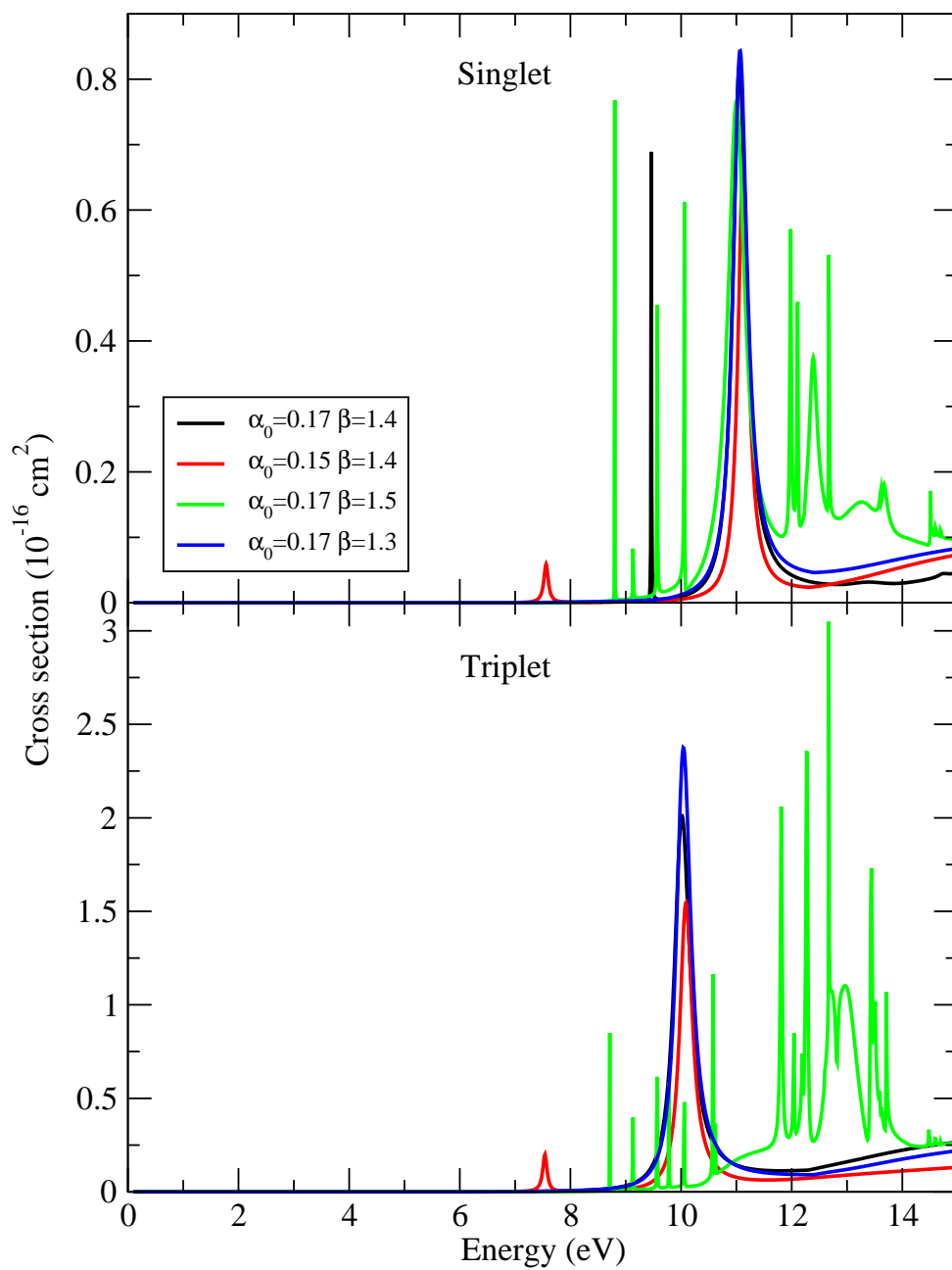


Figure 2. Partial electron impact detachment cross sections of C_2^- for Model 4 for final states of ${}^2B_{3g}$ (${}^2\Pi_g$) total symmetry with different values of (α_0, β) ; ionisation to singlet and triplet final states are shown to illustrate their distinct resonance structures.

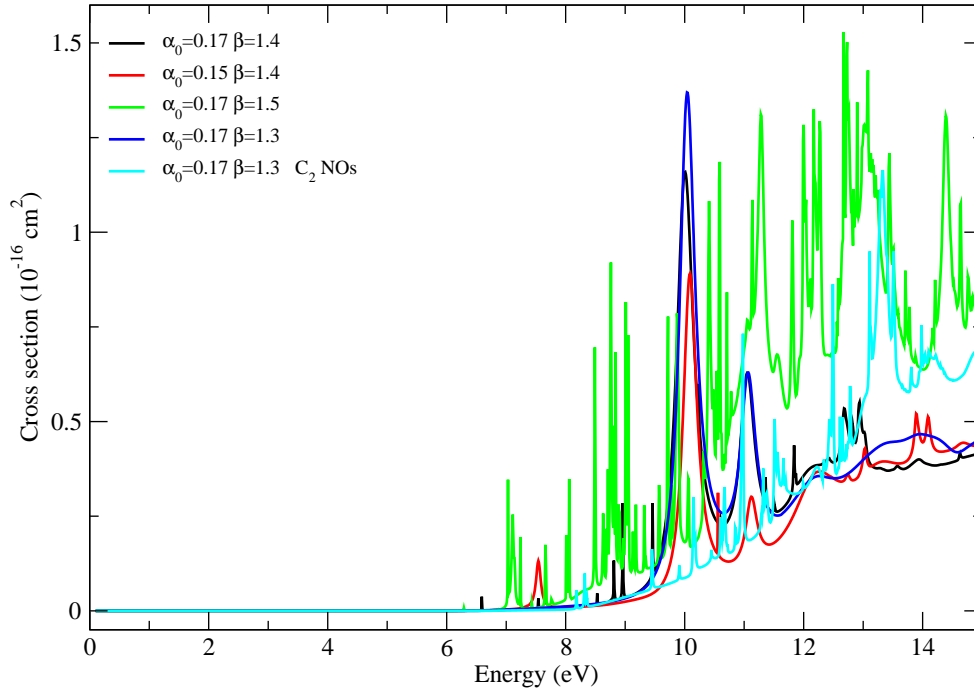


Figure 3. Total electron impact detachment cross sections of C_2^- for Model 4 with different values of (α_0, β) .

a Breit-Wigner formula (Tennyson & Noble 1984). The resulting resonance parameters are given for Model 4 in table 5, where they are compared to previous work.

Sommerfeld et al. (2000) performed careful absorbing potential calculations which found a single $^1\Sigma_g^+$ resonance close the ionisation threshold of C_2^- . We predict a similar resonance, albeit at slightly higher energy; this agreement can be considered satisfactory given the lower level of configuration interaction included in our study. However we find two further resonances not found by Sommerfeld et al. (2000). These resonances lie close in energy to those detected experimentally (Andersen et al. 1996, Pedersen et al. 1998, Pedersen et al. 1999). In fact the experiments give somewhat different resonance characteristics depending on whether they measure the detachment cross section, which gives a width of 2.1 eV, or the smaller dissociation cross section, which gives widths between 3 and 4 eV. However to really test whether these resonances agree it is necessary to make a more direct comparison with the experiments which means comparing with the measured cross sections.

4.2. Cross sections

Figure 4 gives a comparison between our calculations, performed with three different models, and the measurements. What is immediately apparent is that without the Born correction our cross sections are very significantly lower than the measured ones. This supports the assertion made above that the majority of the ionisation occurs through large impact parameter collisions.

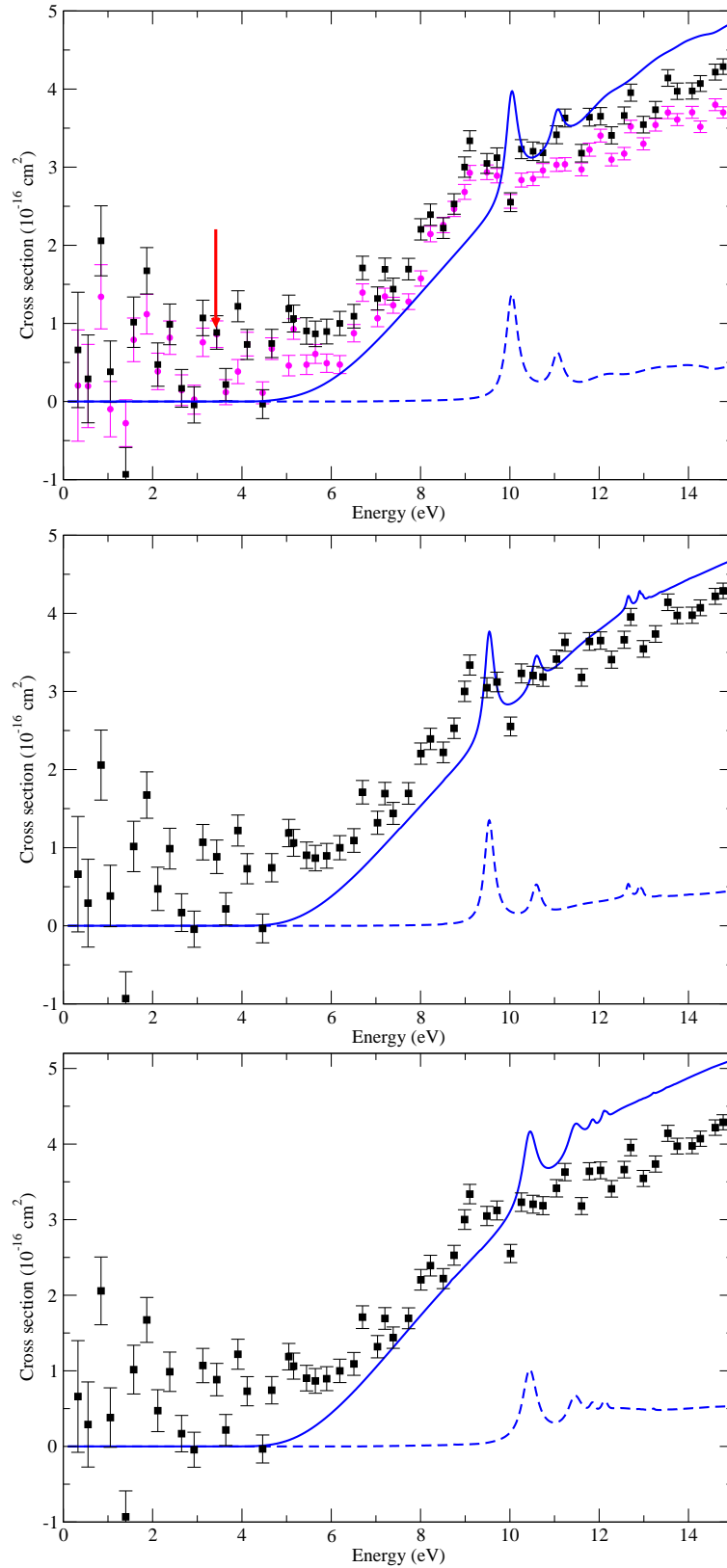


Figure 4. C_2^- electron impact ionisation cross sections. Experimental data due to Pedersen et al. (1999) is given by circles (without dissociative channels) and squares (with dissociative channels); the dashed lines represent our cross sections without Born correction; the solid line represent our cross sections with Born correction. The arrow indicates the location of the ionisation threshold. Top panel: Model 4 with $\alpha_0=0.17$ and $\beta=1.4$; Middle panel: Model 5 with $\alpha_0=0.17$ and $\beta=1.4$; Bottom panel: Model 6 with $\alpha_0=0.17$ and $\beta=1.2$.

All the models shown give reasonable agreement with the measurements of Pedersen et al. (1999). For completeness we give the measured results with and without the consideration of simultaneous ionisation and dissociation. Our calculations implicitly give the cross section for all processes that involve ionisation and therefore should account for both channels. As the dissociation channel is relatively unfavoured, these two measurements are close together, the difference is certainly smaller than the accuracy of our calculations.

It can be seen that all three models give total ionisation cross sections in good agreement with the measurements. In this context it should be noted that the cross sections should all go to zero below the ionisation threshold denoted by the arrow. Furthermore our resonance structures are very similar to, if a little higher in energy than, the observed ones. For reasons discussed for the lower-lying $^1\Sigma_g^+$ resonance, we would expect our resonance energies to be a little too high. This aspect of the agreement can therefore also be considered to be very good.

Finally figure 5 gives total electron impact electronic excitation cross sections for the two bound states of C_2^- . These excitations are both dipole allowed and the cross sections are again completely dominated by the high impact parameter, dipole-driven transitions which we characterise with the Born approximation. Indeed as we predict essentially no resonance structure in these cross sections, a simple Born calculation should suffice for this problem.

5. Discussion and conclusions

Our calculations detect the clear signature of 3 resonances: one of $^1\Sigma_g^+$ symmetry just above the ionisation threshold and resonances with singlet and triplet spin and Π_g spatial symmetry at about 10 eV. Since they all lie above the excited electron states of C_2^- , these must be regarded as shape resonances. The standard model for shape resonances in electron – molecule collisions relies on a centrifugal barrier to provide the trapping potential. Such resonances have two characteristics: they are not found for s-wave scattering and they occur, often at too high an energy, in simple static exchange calculations. The present resonances are absent from the test static exchange calculations we ran and the $^1\Sigma_g^+$ resonance involves s-wave scattering.

All this implies a modified picture of a shape resonance. The situation here is that the scattering occurs under the influence of a strongly repulsive Coulomb potential. The well required to (temporarily) trap the scattering electron should therefore be the result of some local attraction. Our calculations suggest that this is indeed what happens and the attractive component is provided by polarisation interactions. This is why characterising the resonances require such a sophisticated representation of the target wave functions.

Although representation of the resonances requires a very sophisticated treatment of the target, this is not the situation for the cross sections. Both the electron impact electronic excitation and electron detachment cross sections are dominated by long range

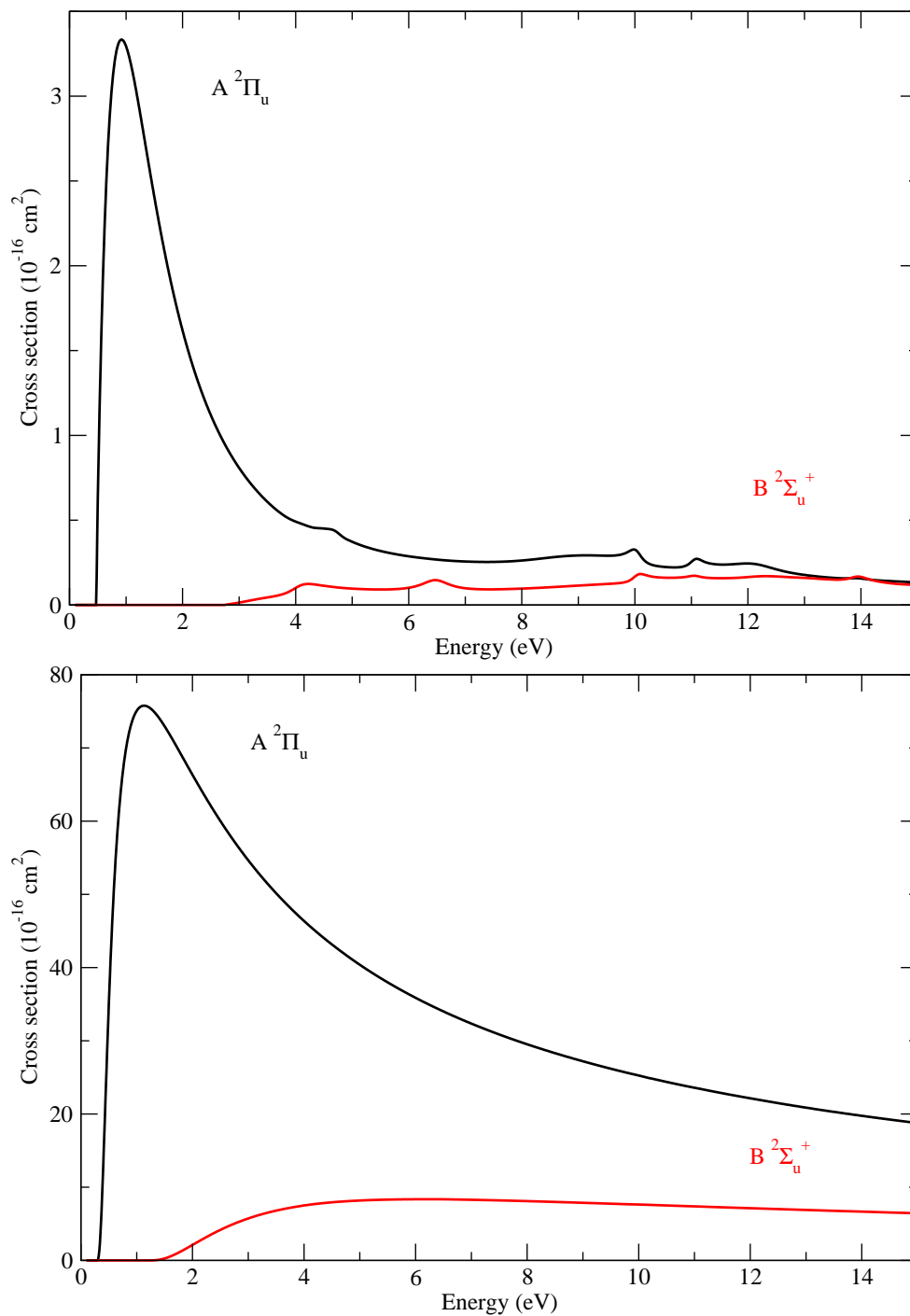


Figure 5. Electron impact electronic excitation cross sections for excitation to the $A^2\Pi_u$ and $B^2\Sigma_u^+$ states without (upper) and with (lower) Born correction; note the very different cross section scales for the two panels. Calculations are for Model 4 with $\alpha_0=0.17$ and $\beta=1.3$.

collisions which can be modelled using a simple Born approximation. It should however be noted that our treatment of the electron impact electron detachment process does involve the use of a discretised continuum via the MRMPS method which is then used to provide the necessary transition dipoles for the Born calculation.

In summary our calculations on electron impact electron detachment of C_2^- reproduce both the resonance structure and cross sections observed over a number of years in storage rings (Andersen et al. 1996, Pedersen et al. 1998, Pedersen et al. 1999) for this process. These calculations are the first to achieve either of these goals. To do this we had to combine a sophisticated treatment of the C_2^- target including representation of target continuum states using the molecular R-matrix with pseudo states (MRMPS) method with a method for calculating the effects of high impact parameter collisions.

References

- Andersen L H, Bak J, Boye S, Clausen M, Jensen M H M J, Lapierre A & Seiersen K 2001 *J. Chem. Phys.* **115**, 3566.
- Andersen L H, Hvelplund P, Kella D, Mokler P H, Pedersen B, Schmidt H T & Vejby-Christensen L 1996 *J. Phys. B: At. Mol. Opt. Phys.* **29**, L643.
- Baluja K L, Mason N J, Morgan L A & Tennyson J 2001 *J. Phys. B: At. Mol. Opt. Phys.* **34**, 2807–2821.
- Bartschat K & Bray I 1996 *J. Phys. B: At. Mol. Opt. Phys.* **29**, L577–L583.
- Bartschat K, Hudson E T, Scott M P, Burke P G & Burke V M 1996 *J. Phys. B: At. Mol. Opt. Phys.* **29**, 115–123.
- Burke P G & Berrington K A, eds 1993 *Atomic and Molecular Processes, an R-matrix Approach* Institute of Physics Publishing Bristol.
- Burke P G & Tennyson J 2005 *Mol. Phys.* **103**, 2537–2548.
- Collins G F, Pegg D J, Fritioff K, Sandström J, Hanstorp D, Thomas R D, Hellberg F, Ehlerding A, Larsson M, Österdahl F, Källberg A & Danared H 2005 *Phys. Rev. A* **72**, 043708.
- Dunning T H 1970 *J. Chem. Phys.* **53**, 2823.
- Faure A, Gorfinkiel J D, Morgan L A & Tennyson J 2002 *Computer Phys. Comms.* **144**, 224–241.
- Gorfinkiel J D & Tennyson J 2004 *J. Phys. B: At. Mol. Opt. Phys.* **37**, L343–L350.
- Gorfinkiel J D & Tennyson J 2005 *J. Phys. B: At. Mol. Opt. Phys.* **38**, 1607–1622.
- Halmová G 2008 R-matrix calculations of electron-molecule collisions with C_2 and C_2^- PhD thesis University College London.
- Halmova G, Gorfinkel J D & Tennyson J 2006 *J. Phys. B: At. Mol. Opt. Phys.* **39**, 2849–2860.
- Halmová G & Tennyson J 2008 (submitted).
- Huber K P & Herzberg G, eds 1979 *Constants of Diatomic Molecules* Van Nostrand Reinhold.
- Morgan L A, Gillan C J, Tennyson J & Chen X 1997 *J. Phys. B: At. Mol. Opt. Phys.* **30**, 4087–4096.
- Pedersen B, Djurić N, Jensen M J, Kella D, Safvan C P, Schmidt H T, Vejby-Christensen L & Andersen L H 1999 *Phys. Rev. A* **60**, 2882.
- Pedersen H B, Djurić N, Jensen M J, Kella D, Safvan C P, Vejby-Christensen L & Andersen L H 1998 *Phys. Rev. Lett.* **81**, 5302.
- Rozum I, Mason N J & Tennyson J 2003 *New J. Phys.* **5**, 1–155.
- Schmidt M W & Ruedenberg K 1979 *J. Chem. Phys.* **71**, 3951.
- Sommerfeld T, Riss U V, Meyer H D & Cederbaum L 1997 *Phys. Rev. Lett.* **79**, 1237.
- Sommerfeld T, Tarantelli F, Meyer H D & Cederbaum L 2000 *J. Chem. Phys.* **112**, 6635.
- Tennyson J 1996a *J. Phys. B: At. Mol. Opt. Phys.* **29**, 1817–1828.
- Tennyson J 1996b *J. Phys. B: At. Mol. Opt. Phys.* **29**, 6185–6201.
- Tennyson J 1997 *Computer Phys. Comms.* **100**, 26–30.
- Tennyson J 2004 *J. Phys. B: At. Mol. Opt. Phys.* **37**, 1061–1071.

Tennyson J & Halmová G 2007 in 'Mathematical and Computational Methods in R-matrix Theory' CCP2, Daresbury pp. 85–90.

Tennyson J & Morgan L A 1999 *Phil. Trans. A* **357**, 1161–1173.

Tennyson J & Noble C J 1984 *Computer Phys. Comms.* **33**, 421–424.